Stabilization of quantum metastable states by dissipation

D. Valenti,[1,*] L. Magazzù,[1,2,†] P. Caldara,[1] and B. Spagnolo[1,2,3,‡]

[1]*Dipartimento di Fisica e Chimica, Group of Interdisciplinary Theoretical Physics, Università di Palermo and CNISM, Unità di Palermo, Viale delle Scienze, Edificio 18, I-90128 Palermo, Italy*

[2]*Radiophysics Department, Lobachevsky State University of Nizhni Novgorod, 23 Gagarin Avenue, Nizhni Novgorod 603950, Russia*

[3]*Istituto Nazionale di Fisica Nucleare, Sezione di Catania, Via S. Sofia 64, I-90123 Catania, Italy*

(Received 29 July 2014; revised manuscript received 26 March 2015; published 10 June 2015)

Normally, quantum fluctuations enhance the escape from metastable states in the presence of dissipation. Here we show that dissipation can enhance the stability of a quantum metastable system, consisting of a particle moving in a strongly asymmetric double well potential, interacting with a thermal bath. We find that the escape time from the metastable region has a nonmonotonic behavior versus the system-bath coupling and the temperature, producing a stabilizing effect.

DOI: 10.1103/PhysRevB.91.235412 PACS number(s): 03.65.Xp, 03.65.Aa, 03.65.Db, 03.65.Yz

I. INTRODUCTION

Recently, the role of dissipation on the dynamics of quantum systems has been the subject of renewed interest [1].

The presence of a dissipative environment indeed significantly influences the escape from a quantum metastable state. This is a general problem, of interest in many areas of physics, whenever a sudden change in the state of a system occurs on time scales small with respect to the typical times of the systems dynamics.

The archetypical model describing the escape process is that of a particle subject to a cubic or asymmetric bistable potential and linearly coupled to a heat bath of quantum harmonic oscillators [2–4]. In such a system the decay from the metastable state occurs on time scales that depend on the friction and temperature. Various physical systems such as magnetization in solid state systems [5], proton transfer in chemical reactions [6], and superconducting devices [7] can be described within this framework.

Calculations of the decay rates, using a cubic potential, have been performed in Refs. [8,9] using functional integral techniques. In Ref. [9], starting with the particle at the bottom of the metastable well, it has been shown that the decay rate decreases monotonically as the damping increases and grows with the bath temperature. Similarly, by using a master equation technique, a monotonic increase of the escape rate, with respect to the temperature, is found in Ref. [10] for a Gaussian wave packet initially in the metastable well of a biased quartic potential.

Stabilization of a quantum metastable state by an external time-periodic driving, in absence of environment, was obtained in Ref. [11]. Moreover, suppression of activated escape from a metastable state by increasing the temperature was found in a time-periodically driven quantum dissipative system [12].

Common wisdom is that environmental fluctuations always enhance the escape from a quantum metastable state. A critical issue of great importance is whether the dissipation can enhance the stability of a quantum metastable state.

To answer this question we follow the time evolution of the populations of spatially localized states in a strongly asymmetric bistable system, starting from a nonequilibrium initial condition. This choice allows us to observe how, increasing the damping, the relaxation process towards the stable well goes from a population transfer in which the metastable well is temporarily populated, to a mechanism of direct transfer to the stable state. This stabilization effect is related to the suppression of tunneling by dissipation in quantum regime [2,9]. As a result we find that dissipation can enhance the stability of the quantum metastable state. Indeed, we observe that the escape dynamics is characterized by a nonmonotonic behavior, with a maximum, as a function of the damping strength: there is an optimal value of the damping strength which maximizes the escape time, producing a *stabilizing* effect in the quantum system. This result resembles the phenomenon known, in the classical context, as noise enhanced stability (NES) of metastable states [13–16]. We also find that the behavior of the escape time versus the temperature is nonmonotonic, and in particular is characterized by the presence of a minimum. Therefore, as the temperature increases, an enhancement of the escape time is observed, increasing the stability of the metastable state. These results shed new light on the role of the environmental fluctuations in stabilizing quantum metastable systems.

For classical systems, several theoretical studies show that the average escape time from metastable states in the presence of fluctuating and static potentials is characterized by nonmonotonicity with respect to the noise intensity D [14–19]. This resonancelike behavior, called NES, is in contrast with the monotonic behavior predicted by Kramers theory [20,21]: the stability of metastable or unstable states is in fact enhanced by the noise with the average lifetime resulting larger than the deterministic one. For a classical Brownian particle in a cubic potential, the mean first passage time (MFPT) as a function of D is characterized by a maximum when the particle is placed initially outside the metastable well, in a certain region on the right of the potential maximum, that is in a nonequilibrium position. For very low noise intensities, in the limit $D \to 0$, the MFPT diverges as a consequence of the trapping of the Brownian particle in the potential well [14,16]. Increasing the value of D, the particle can escape out more easily and the MFPT decreases. As the noise intensity reaches a value

*davide.valenti@unipa.it
†luca.magazzu@unipa.it
‡bernardo.spagnolo@unipa.it

$D \approx \Delta U$, with ΔU the potential barrier height, the escape process of the Brownian particle is slowed down, due to the fact that the probability to reenter the well is increased. At higher noise intensities, one recovers a monotonic decreasing behavior of the MFPT. In summary, the behavior of the MFPT vs D goes with continuity from a monotonic divergent behavior to a nonmonotonic finite behavior (typical NES effect), passing through a nonmonotonic divergent behavior with a minimum and a maximum [16].

In this work we extend the investigation on the stabilizing effects of the noise to the quantum context, studying the dissipative dynamics of the quantum system introduced above, i.e., a quantum particle moving along an asymmetric bistable potential.

II. MODEL

We consider a quantum *particle* of effective mass M in a double well potential (see Fig. 1). The system's bare Hamiltonian is $\hat{H}_0 = \hat{p}^2/2M + V(\hat{q})$, where

$$V(\hat{q}) = \frac{M^2\omega_0^4}{64\Delta U}\hat{q}^4 - \frac{M\omega_0^2}{4}\hat{q}^2 - \hat{q}\epsilon. \tag{1}$$

Here ω_0 is the natural oscillation frequency around the minima, ΔU is the barrier height, and ϵ is the asymmetry parameter. In this work ϵ is large enough to mimic the cubic potential, which is the archetypal model potential for metastable systems.

The environment is a thermal bath of N independent harmonic oscillators with position coordinates $\hat{x}_j$ and coupled with the particle through the linear interaction term $\sum_{j=1}^{N} c_j \hat{x}_j \hat{q}$.

In our study it is assumed that, in the continuum limit $N \to \infty$, the bath has the Ohmic spectral density $J(\omega) = M\gamma\omega$ with a cutoff at a frequency much larger than any other involved in the model. The damping constant γ is a measure of the overall particle-bath coupling strength and has the same role as the classical damping in the quantum Langevin equation associated to the present problem [4].

In the quantum regime, given the particle's initial preparation, the bath temperature is such that the dynamics is practically confined among the first six levels of the potential shown in Fig. 1. In this reduced Hilbert space, performing a suitable transformation, we pass to the discrete variable representation (DVR) [22], in which the particle's reduced dynamics is described in terms of the *localized* basis of the position eigenstates $\{|q_1\rangle, \ldots, |q_6\rangle\}$, where $\hat{q}|q_i\rangle = q_i|q_i\rangle$.

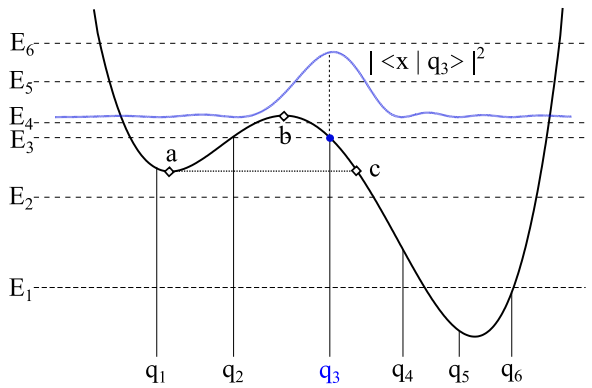

FIG. 1. (Color online) Potential $V(q)$ of Eq. (1), with $\Delta U = 1.4\hbar\omega_0$ and $\epsilon = 0.27\sqrt{M\hbar\omega_0^3}$. Horizontal lines: the first six energy levels. Vertical lines: the position eigenvalues in the DVR. The dashed curve is the initial probability density $|\Psi(x,0)|^2$. For the tunneling splitting we have $\Delta E_{4,3} = E_4 - E_3 = 0.2\hbar\omega_0$, while $E_2 - E_1 = 0.985\hbar\omega_0$. The initial condition q_3 is the highlighted by a blue point.

III. ANALYTICAL METHOD

We assume a factorized initial condition, with the bath in the thermal state $\rho_B(0) = e^{-\beta\hat{H}_B}/Z_B$. The particle's reduced density operator in the DVR is given by

$$\rho_{\mu\nu}(t) = \sum_{\alpha,\beta=1}^{6} K(q_\mu,q_\nu,t;q_\alpha,q_\beta,0)\rho_{\alpha\beta}(0), \tag{2}$$

where $\rho_{\mu\nu}(t) = \langle q_\mu|\rho(t)|q_\nu\rangle$ $(\mu,\nu = 1,\ldots,6)$ and $K(q_\mu,q_\nu,t;q_\alpha,q_\beta,0)$ is given by the double dissipative path integral

$$\int_{q_\alpha}^{q_\mu} \mathcal{D}q(t) \int_{q_\beta}^{q_\nu} \mathcal{D}^* q'(t) \mathcal{A}[q]\mathcal{A}^*[q']\mathcal{F}_{FV}[q,q']. \tag{3}$$

Here $\mathcal{A}[q]$ is the amplitude associated with the path $q(t)$ of the bare system. In the DVR a path is a steplike function with transitions among the positions q_i. The effect exerted by the bath on the quantum-mechanical amplitude associated to a path $(q(t),q'(t))$ is condensed in the Feynman-Vernon (FV) influence functional $\mathcal{F}_{FV}[q,q']$ [23].

This approach is nonperturbative in the system-bath coupling, and is thus suited for dealing with the strong-coupling regime. Nevertheless, the FV influence functional makes the path integral intractable as it introduces time nonlocal *interactions* between the paths $q(t)$ and $q'(t)$, through the bath correlation function $Q(t)$.

The nonlocal part of the interactions cancels out in the limit in which the bath correlation function $Q(t)$ is linear in t, i.e. in the long time limit $t \gg \hbar/k_BT$ (see Sec. IV and Appendix B in Ref. [24]). If the temperature is sufficiently high, $Q(t)$ can be taken in the linearized form at all times, which amounts to performing the so-called *generalized noninteracting cluster approximation* (gNICA [24], the multilevel version of the noninteracting blip approximation for the spin-boson model [2,4]). By comparing the transition probabilities per unit time among the $|q_i\rangle$'s with $k_BT/\hbar$, we obtain the limit $T \gtrsim 0.1\hbar\omega_0/k_B$ as a rough estimate for the validity of the gNICA for our system.

Within the gNICA the double path integral of Eq. (3) assumes a factorized form in the Laplace space, allowing for the derivation of a generalized master equation (GME). If $\rho(0)$ is diagonal in the position representation, the GME reads [24]

$$\dot{\rho}_{\mu\mu}(t) = \sum_{\nu=1}^{6} \int_0^t dt' \mathcal{H}_{\mu\nu}(t-t')\rho_{\nu\nu}(t'). \tag{4}$$

The elements of $\mathcal{H}$ are taken to the second order in the transition amplitudes per unit time $\Delta_{ij} = \langle q_i|\hat{H}_0|q_j\rangle/\hbar$ and at all orders in the system-bath coupling. They display a cutoff of the type $\exp(-\gamma t \times \text{const})$. At strong damping (as in our case, see below), in the short time interval in which $\mathcal{H}_{\mu\nu}$ is substantially different from zero, $\rho_{\nu\nu}(t)$ are practically constant. This allows us to write the following rate equation

as the Markov approximated version of Eq. (4):

$$\dot{\rho}_{\mu\mu}(t) = \sum_{\nu=1}^{6} \Gamma_{\mu\nu}\rho_{\nu\nu}(t), \tag{5}$$

where $\Gamma_{\mu\nu} = \int_0^\infty d\tau \mathcal{H}_{\mu\nu}(\tau)$.

The smallest, in absolute value, of the nonzero eigenvalues of the rate matrix Γ determines the largest time scale of the dynamics, that is, the quantum relaxation time $\tau_{\rm relax}$ [24].

IV. ESCAPE TIME

In the following we focus on the particle's transient dynamics, as given by the solution of Eq. (5) with the nonequilibrium initial condition

$$\rho(0) = |q_3\rangle\langle q_3|, \tag{6}$$

i.e., with the particle's probability density initially peaked on the right of the potential barrier, in the interval (q_b,q_c), where q_c is the *exit point* (see Fig. 1 and Ref. [4]). This initial condition may be experimentally attained by preparing the particle in the ground state of an appropriate harmonic well centered at the desired position, and then releasing the harmonic potential [25].

The out-of-equilibrium initial condition considered in this work is qualitatively different from the quasistationary state considered in Ref. [9], and references therein, where the particle is in the ground state of a metastable cubic potential. The decay rate calculated there gives information on the time the particle takes to leave the metastable well starting from the quasistationary state.

The thermodynamical method used there [9] is not suited for treating out-of-equilibrium dynamics. To this aim we introduce an escape time which is suitable to describe out-of-equilibrium dynamics in bistable quantum systems, and closely resembling the escape problem in classical statistical physics [13–15].

Processes starting from nonequilibrium initial conditions are commonly encountered in nature, at the classical and quantum scale (see Refs. [26,27], and references therein). A typical example of nonequilibrium dynamics is that emerging from a sudden quenching [27].

Before giving the definition of escape time in the present context, we define the population of the lower (right side) well as the cumulative population of the three DVR states from $|q_4\rangle$ to $|q_6\rangle$, that is,

$$P_{\rm right}(t) = \sum_{\mu=4}^{6} \rho_{\mu\mu}(t), \tag{7}$$

which is a discretized version of the probability of penetration of the wave packet through the barrier [10]. During the transient dynamics the populations of the metastable states ($|q_1\rangle$ and $|q_2\rangle$) reach a maximum. Afterwards, by tunneling through the potential barrier, the population of the metastable well decays, finally settling down to a stationary value dependent on the temperature.

We note that actually we calculate the escape time from the *metastable region*, which we define as the region to the left of the *exit point* q_c (see Fig. 1 and p. 190 of Ref. [4]), therefore comprising the metastable well.

We consider large asymmetry of the potential, low temperatures with respect to the barrier height, and damping regimes ranging from moderate to strong ($\gamma \gtrsim \omega_0$). Given the above conditions, the relaxation occurs in the incoherent regime, with no oscillations in the populations [24]. As a consequence we may consider the particle irreversibly out of the metastable region once $P_{\rm right}(t)$ has reached a certain threshold value that we set to $P_{\rm right}(\tau) = 0.95$.

V. RESULTS

Figure 2 shows the presence of a peak in τ vs γ, whose height and position depend on the temperature.

A comparison between τ and $\tau_{\rm relax}$ versus γ indicates that the two quantities exhibit roughly the same behavior until the peak in τ is reached [see Fig. 2(b)]. At higher γ, while $\tau_{\rm relax}$ continues to increase monotonically, τ has a sudden fall off at a critical value γ_c, dependent on the temperature (for example, $\gamma_c \simeq 0.98$ at $T = 0.352$).

This critical value corresponds to a dynamical regime in which the population transfer from the initial state to the states of the metastable well is inhibited and there is a direct transfer to the states of the lower right well. In this regime the probability of finding the particle in the metastable region is

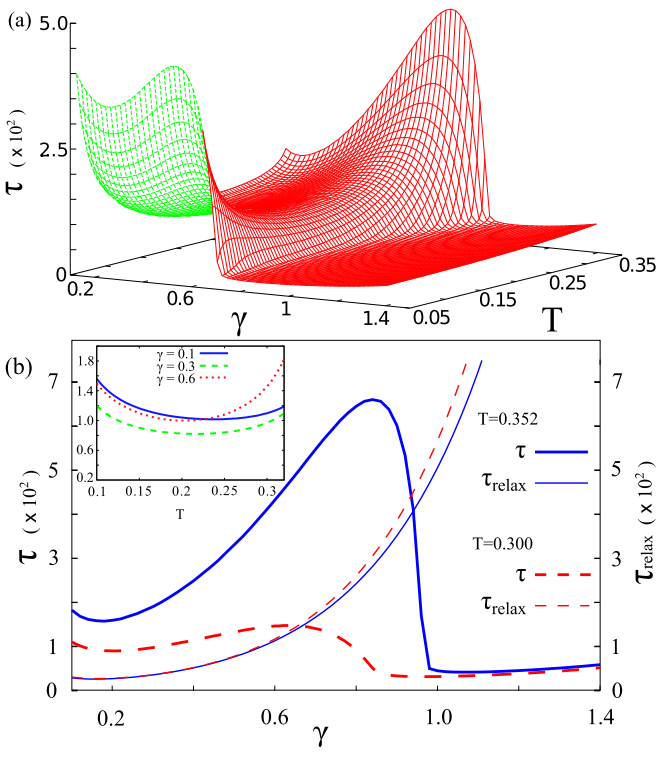

FIG. 2. (Color online) Escape time τ, in units of ω_0^{-1}, for the initial condition $\rho(0) = |q_3\rangle\langle q_3|$ [see Eq. (6)]. (a) τ as a function of both damping γ and temperature T, with threshold 0.95. (b) τ and $\tau_{\rm relax}$ as functions of γ for different temperatures, namely, $T = 0.3, 0.352$. Inset: Escape time vs temperature at fixed values of damping, namely, $\gamma = 0.1, 0.3, 0.6$. The parameters γ and T are given in units of ω_0 and $\hbar\omega_0/k_B$, respectively.

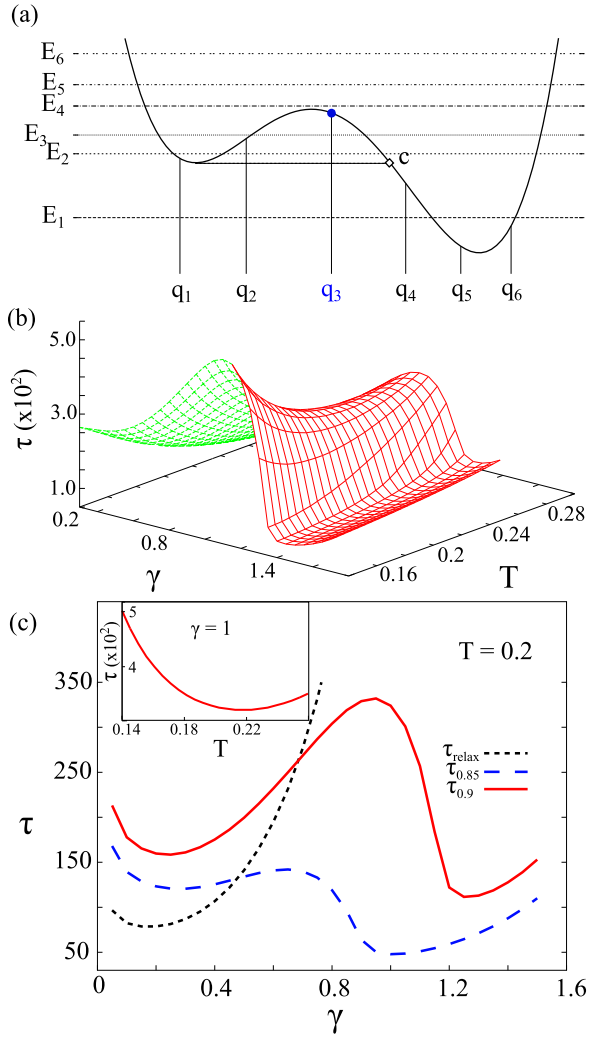

FIG. 3. (Color online) (a) Potential $V(q)$ ($\Delta U = 1.4\hbar\omega_0$ and $\epsilon = 0.2\sqrt{M\hbar\omega_0^3}$, slightly more symmetric than that in Fig. 1) with the first $M = 6$ energy levels E_i (horizontal lines) and corresponding position eigenvalues q_i in the DVR (vertical lines). (b) Escape time τ, in units of ω_0^{-1}, vs γ and T for the threshold 0.9. (c) Escape time τ (for two different thresholds) and relaxation time $\tau_{\rm relax}$ vs the damping strength γ at $T = 0.2$. Both in (b) and (c) the particle is initially *localized* around q_3 [blue point in (a)]. The parameters γ and T are given in units of ω_0 and $\hbar\omega_0/k_B$, respectively.

practically zero throughout the entire dynamics. Indeed, while $\tau_{\rm relax}$ is the time needed for the system to reach the equilibrium in the double well potential, the escape time is a relevant quantity for the transient dynamics, involving the crossing of the potential barrier and the emptying of the metastable well. Therefore, our analysis applies to the general problem of escape from a metastable well, starting from a nonequilibrium condition.

The nonmonotonic behavior of τ vs γ can be interpreted as the quantum counterpart of the NES phenomenon observed in classical systems, and may be called quantum noise enhanced stability (QNES).

Another interesting feature is the presence of a slow monotonic increase of τ for $\gamma > \gamma_c$, which leads to the quantum Zeno effect [28].

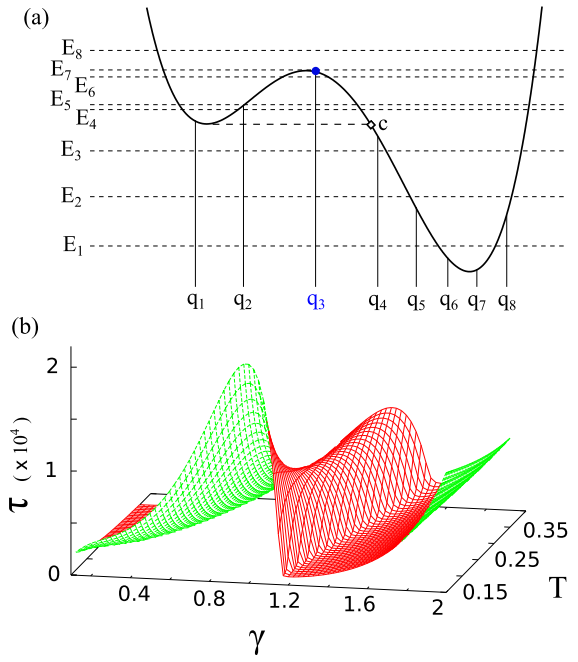

FIG. 4. (Color online) (a) Potential $V(q)$ of Eq. (1), with $\Delta U = 2.5\hbar\omega_0$ and $\epsilon = 0.35\sqrt{M\hbar\omega_0^3}$. Horizontal lines: the first eight energy levels. Vertical lines: position eigenvalues in the DVR. The dashed curve is the initial probability density $|\Psi(x,0)|^2$. Here $\Delta E_{7,6} = 0.14\hbar\omega_0$, $\Delta E_{6,5} = 0.58\hbar\omega_0$, and $\Delta E_{5,4} = 0.1\hbar\omega_0$. (b) Escape time τ, in units of ω_0^{-1}, as a function of both γ and T for the initial condition q_3 (blue point) shown in panel (a). The parameters γ and T are given in units of ω_0 and $\hbar\omega_0/k_B$, respectively. The threshold value is 0.95.

The behavior of τ vs the temperature is characterized by a minimum as k_BT approaches the tunneling splitting $\Delta E_{4,3} = E_4 - E_3 = 0.2\hbar\omega_0$ (see Fig. 1). This is the signature of the *thermally activated tunneling*, an experimentally well established phenomenon [29]. This is better shown in the inset of Fig. 2(b).

We wish to point out that our results are robust against the variation of the potential asymmetry, threshold value, initial conditions [initial DVR states within the interval (q_b,q_c); see Figs. 3–8], and the dimension of the reduced Hilbert space of the system.

The path integral approach within the DVR is not spatially continuous: the spatial continuity is recovered in the limit of infinitely many energy levels. Nevertheless, by increasing gradually the number M of energy states taken into account in our approximation of the M-state system, the DVR states change their "localization" and become more dense, especially in the regions where the potential energy is lower (inside the two wells). This means that enlarging the Hilbert space considered, new DVR states with different eigenvalues in the interval (q_b,q_c) can be used as initial conditions.

In what follows we show that a qualitatively similar behavior of the escape time τ vs γ and T, as that shown in Fig. 2, is present changing the potential asymmetry, the threshold values, the number M of energy states considered, and the initial localization of the particle in the nonequilibrium region between the top of the potential barrier and the exit point q_c.

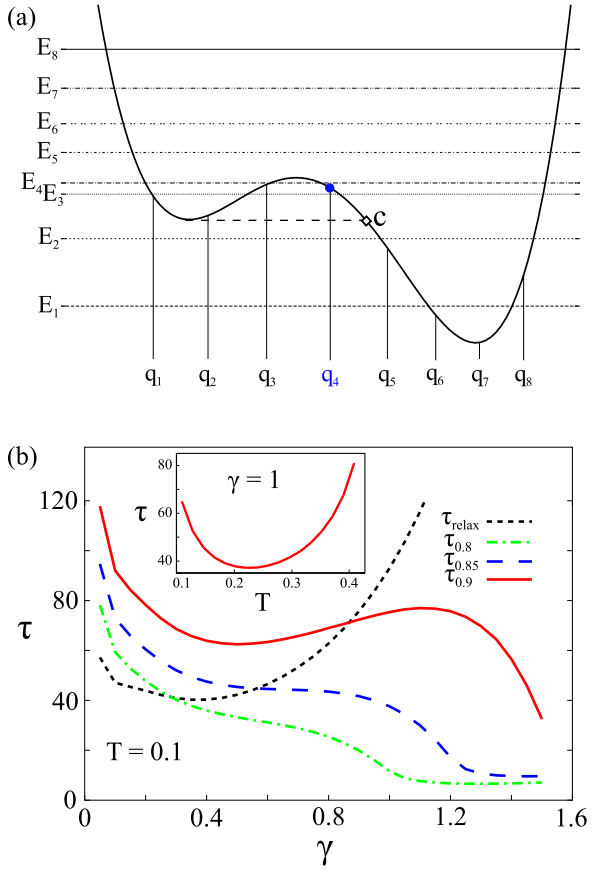

FIG. 5. (Color online) (a) Potential $V(q)$ ($\Delta U = 1.4\hbar\omega_0$ and $\epsilon = 0.27\sqrt{M\hbar\omega_0^3}$, the same as in Fig. 1) with the first $M = 8$ energy levels E_i (horizontal lines) and corresponding position eigenvalues q_i in the DVR (vertical lines). (b) Escape time τ at various thresholds (0.8,0.85,0.9) and relaxation time $\tau_{\rm relax}$, both in units of ω_0^{-1}, vs the damping strength γ at $T = 0.1$. Inset: τ vs T at $\gamma = 1$. The particle is initially in the state $|q_4\rangle$, i.e., *localized* around q_4 [blue point in (a)]. The parameters γ and T are given in units of ω_0 and $\hbar\omega_0/k_B$, respectively.

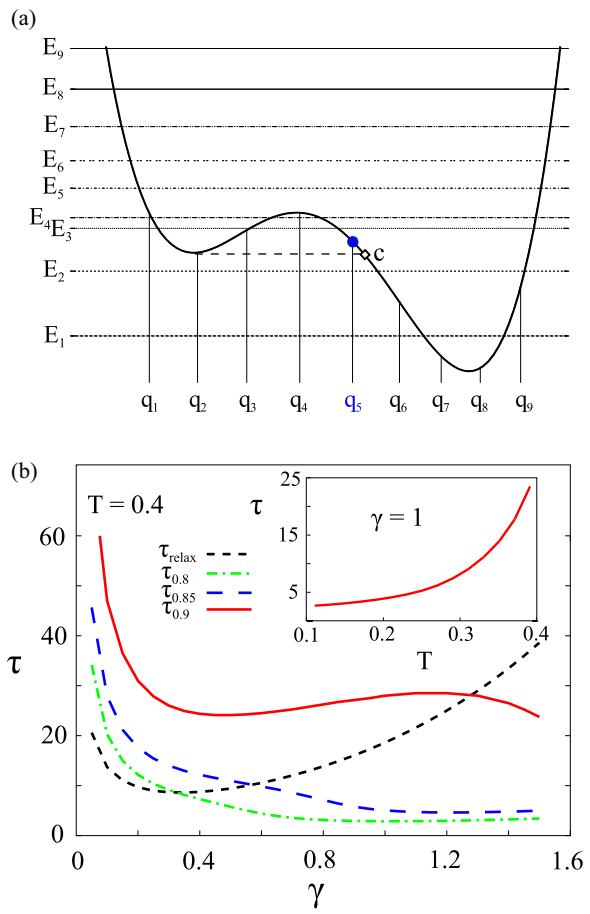

FIG. 6. (Color online) (a) Potential $V(q)$ ($\Delta U = 1.4\hbar\omega_0$ and $\epsilon = 0.27\sqrt{M\hbar\omega_0^3}$, the same as in Fig. 1) with the first $M = 9$ energy levels E_i (horizontal lines) and corresponding position eigenvalues q_i in the DVR (vertical lines). (b) Escape time τ at various thresholds (0.8,0.85,0.9) and relaxation time $\tau_{\rm relax}$, both in units of ω_0^{-1}, vs the damping strength γ at $T = 0.4$. Inset: τ vs T at $\gamma = 1$. The particle is initially *localized* around q_5 [blue point in (a)]. The parameters γ and T are given in units of ω_0 and $\hbar\omega_0/k_B$, respectively.

In Fig. 3 we show the results for the escape time with threshold 0.9 as a function of both the damping strength and the temperature, using a different, more symmetric, potential with $\epsilon = 0.2\sqrt{M\hbar\omega_0^3}$ (in Fig. 2 the asymmetry parameter is $\epsilon = 0.27\sqrt{M\hbar\omega_0^3}$). With this choice the initial state $|q_3\rangle$ is localized nearer the potential top with respect to the previous case (Fig. 1). We find that the nonmonotonic behavior of the escape time with respect to γ is present also in this case, with a peak followed by a monotonic increase. A minimum with respect to the temperature is also present as $k_B T$ approaches the tunneling splitting $E_3 - E_2 \sim 0.27\hbar\omega_0$.

We also provide, in Fig. 4, the escape time vs γ and T in the case of a *more* asymmetric potential ($\epsilon = 0.35\sqrt{M\hbar\omega_0^3}$) with respect to that of Fig. 1, and considering $M = 8$ energy levels. Again, the nonequilibrium initial condition is a wave packet centered close to the top of the potential barrier (compare with Fig. 1). The definition of τ is the same as for the first case, i.e., $P_{\rm right}(\tau) = 0.95$. However, due to the different number of energy levels considered, the right well population is now defined as $P_{\rm right}(t) = \sum_{\mu=5}^{8} \rho_{\mu\mu}(t)$.

The escape time displays qualitatively the same features as for the first configuration. In particular, τ has a nonmonotonic behavior as a function of both γ and T. The minimum of τ vs T is at $T \simeq 0.27\hbar\omega_0/k_B$, which is the average value of the three tunneling splittings $\Delta E_{7,6}$, $\Delta E_{6,5}$, and $\Delta E_{5,4}$ [see Fig. 4(a)]. Moreover, for $\gamma > \gamma_c$ we observe a monotonic increasing behavior of τ leading to the quantum Zeno effect.

Next we consider a series of results obtained with the same potential profile as in Fig. 1, but changing the number of energy levels and, as a consequence, the spatial configurations of the DVR states. This, in turn, allows us to consider new initial conditions with localized wave packets within the interval of interest, leaving the potential unchanged. Specifically we consider $M = 8$, 9, and 10 and, in each of these cases, the escape time is defined with the three thresholds 0.8, 0.85, and 0.9. A nonmonotonic behavior of the escape time with respect to the damping parameter, similar to that described above, is observed in all three representations. This is shown in Figs. 5–7. The minima in the T dependence are present for $M = 8$ and 10 at $T \sim 0.21\hbar\omega_0/k_B$, corresponding to the

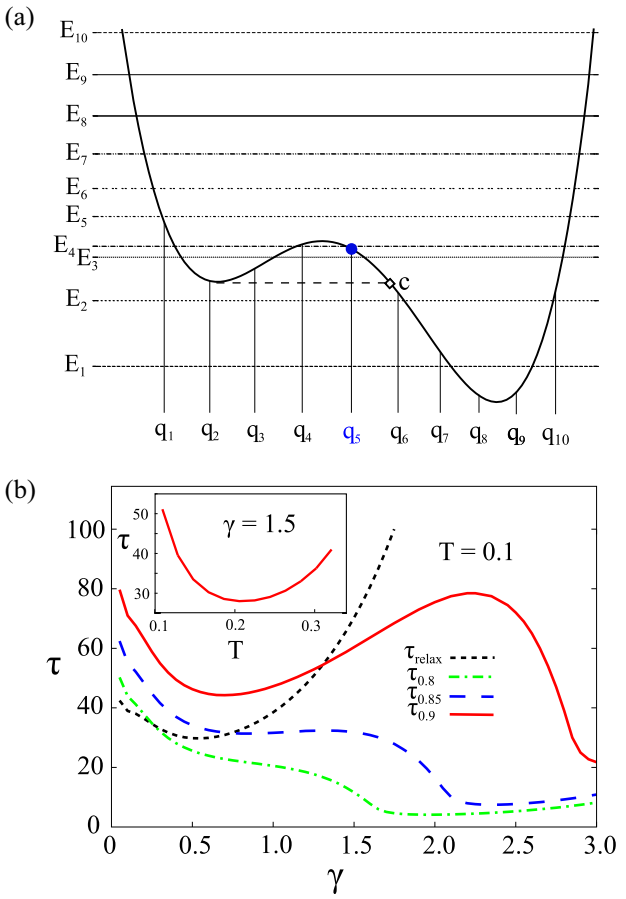

FIG. 7. (Color online) (a) Potential $V(q)$ ($\Delta U = 1.4\hbar\omega_0$ and $\epsilon = 0.27\sqrt{M\hbar\omega_0^3}$, the same as in Fig. 1) with the first $M = 10$ energy levels E_i (horizontal lines) and corresponding position eigenvalues q_i in the DVR (vertical lines). (b) Escape time τ at various thresholds (0.8,0.85,0.9) and relaxation time $\tau_{\rm relax}$, both in units of ω_0^{-1}, vs the damping strength γ at $T = 0.1$. Inset: τ vs T at $\gamma = 1.5$. The particle is initially *localized* around q_5 [blue point in (a)]. The parameters γ and T are given in units of ω_0 and $\hbar\omega_0/k_B$, respectively.

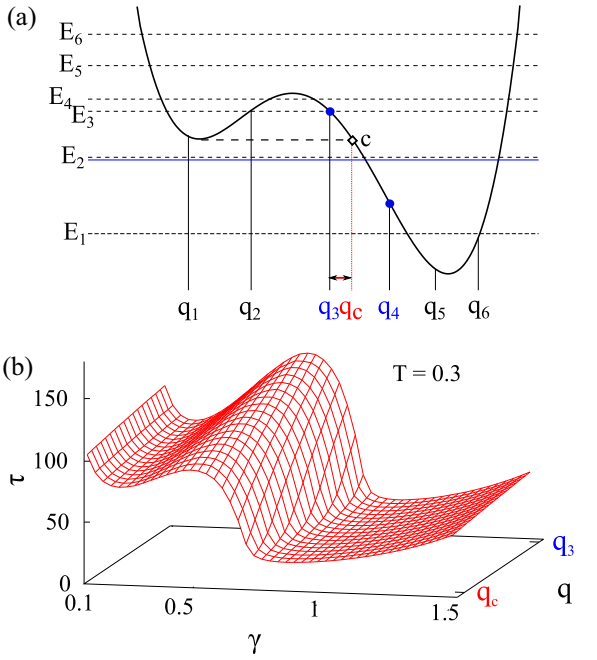

FIG. 8. (Color online) (a) Potential $V(q)$ ($\Delta U = 1.4\hbar\omega_0$ and $\epsilon = 0.27\sqrt{M\hbar\omega_0^3}$, the same as in Fig. 1) with the first $M = 6$ energy levels E_i (horizontal lines) and corresponding position eigenvalues q_i in the DVR (vertical lines). (b) Escape time τ, in units of ω_0^{-1}, as a function of both the damping strength γ and the initial condition, for threshold value equal to 0.95 and temperature $T = 0.3$. The initial conditions are taken as a statistical mixture of $|q_3\rangle$ and $|q_4\rangle$ (blue points), with average positions between q_3 and q_c [see Eq. (8)]. The parameters γ and T are given in units of ω_0 and $\hbar\omega_0/k_B$, respectively.

tunneling splitting $E_4 - E_3 = 0.2\hbar\omega_0$. For $M = 9$ we find a monotonic increase of τ vs T (see inset in Fig. 6). This can be ascribed to the fact that the initial wave packet is localized near the exit point q_c.

In Fig. 8 we show a three-dimensional plot of the escape time, for $M = 6$, as a function of both the damping strength and initial condition, at the fixed temperature $T = 0.3\hbar\omega_0/k_B$. The threshold is set at 0.95. The initial condition is chosen as the statistical mixture

$$\rho(0) = (1 - a)|q_3\rangle\langle q_3| + a|q_4\rangle\langle q_4|, \qquad (8)$$

where the parameter a varies such that the average initial position is in the interval (q_3,q_c). Again, we recover the enhancement of the escape time as a function of γ in the entire range of initial conditions considered.

VI. SUMMARY

We have found that in nonequilibrium dynamics the escape time from a quantum metastable state exhibits a nonmonotonic behavior as a function of both the damping, with a maximum (QNES, see Figs. 2–8), and the temperature, with a minimum at the resonance with the tunneling splitting (see Figs. 1–5 and 7).

Notice that, even though the physics involved in the dissipative tunneling dynamics is the same as that described by the Caldeira-Leggett theory, our study is focused on the out-of-equilibrium initial condition (particle to the right of the potential barrier). In particular, the study is carried out by defining a suitable escape time from the metastable region, the region to the left of the exit point of the potential, and analyzing its behavior as a function of the dissipation parameters.

We observe stabilization of the quantum metastable state due to the damping and its interplay with the temperature, in the moderate to strong damping regime. Moreover, a suppression of the activated escape is obtained by increasing the temperature. The stabilization phenomenon associated to our model is within the reach of existing experimental technologies such as superconducting qubits [25] and optical trapping [30].

The present model could be used to control the stability of a trapped particle in atomic optics, precision spectroscopy, and optical communication.

ACKNOWLEDGMENT

This work was partially supported by MIUR through Grant. No. PON02_00355_3391233, "Tecnologie per l'ENERGia e l'Efficienza energETICa – ENERGETIC".

[1] D. Kast and J. Ankerhold, Phys. Rev. Lett. **110**, 010402 (2013); S. Bera, S. Florens, H. U. Baranger, N. Roch, A. Nazir, and A. W. Chin, Phys. Rev. B **89**, 121108(R) (2014).

[2] A. O. Caldeira and A. J. Leggett, Phys. Rev. Lett. **46**, 211 (1981); A. J. Leggett, S. Chakravarty, A. T. Dorsey, M. P. A. Fisher, A. Garg, and W. Zwerger, Rev. Mod. Phys. **59**, 1 (1987).

[3] M. Grifoni and P. Hänggi, Phys. Rep. **304**, 229 (1998).

[4] U. Weiss, *Quantum Dissipative Systems* (World Scientific, Singapore, 2008).

[5] D. Gatteschi and R. Sessoli, Angew. Chem., Int. Ed. Engl. **42**, 268 (2003); M. N. Leuenberger and D. Loss, Nature (London) **410**, 789 (2001).

[6] H. Naundorf, K. Sundermann, and O. Kühn, Chem. Phys. **240**, 163 (1999).

[7] J. Q. You and F. Nori, Nature (London) **474**, 589 (2011); M. H. Devoret and R. J. Schoelkopf, Science **339**, 1169 (2013).

[8] I. Affleck, Phys. Rev. Lett. **46**, 388 (1981); D. Waxman and A. J. Leggett, Phys. Rev. B **32**, 4450 (1985).

[9] H. Grabert, P. Olschowski, and U. Weiss, Phys. Rev. B **36**, 1931 (1987).

[10] V. V. Sargsyan, Yu. V. Palchikov, Z. Kanokov, G. G. Adamian, and N. V. Antonenko, Phys. Rev. A **75**, 062115 (2007).

[11] C.-L. Ho and C.-C. Lee, Phys. Rev. A **71**, 012102 (2005).

[12] A. Shit, S. Chattopadhyay, and J. Chaudhuri, J. Phys. Chem. A **117**, 8576 (2013); Chem. Phys. **431**, 26 (2014).

[13] R. N. Mantegna and B. Spagnolo, Phys. Rev. Lett. **76**, 563 (1996).

[14] N. V. Agudov and B. Spagnolo, Phys. Rev. E **64**, 035102(R) (2001).

[15] A. A. Dubkov, N. V. Agudov, and B. Spagnolo, Phys. Rev. E **69**, 061103 (2004).

[16] A. Fiasconaro, B. Spagnolo, and S. Boccaletti, Phys. Rev. E **72**, 061110 (2005).

[17] A. Fiasconaro and B. Spagnolo, Phys. Rev. E **80**, 041110 (2009); A. Fiasconaro, J. J. Mazo, and B. Spagnolo, *ibid.* **82**, 041120 (2010).

[18] N. V. Agudov and A. N. Malakhov, Phys. Rev. E **60**, 6333 (1999); D. Dan, M. C. Mahato, and A. M. Jayannavar, *ibid.* **60**, 6421 (1999); R. Wackerbauer, *ibid.* **59**, 2872 (1999); A. Mielke, Phys. Rev. Lett. **84**, 818 (2000).

[19] A. L. Pankratov and B. Spagnolo, Phys. Rev. Lett. **93**, 177001 (2004); P. D'Odorico, F. Laio, and L. Ridolfi, Proc. Natl. Acad. Sci. USA **102**, 10819 (2005); P. I. Hurtado, J. Marro, and P. L. Garrido, Phys. Rev. E **74**, 050101 (2006); J.-H. Li and J. Łuczka, *ibid.* **82**, 041104 (2010); A. A. Smirnov and A. L. Pankratov, Phys. Rev. B **82**, 132405 (2010); Z.-L. Jia and D.-C. Mei, J. Stat. Mech. (2011) P10010; M. Parker, A. Kamenev, and B. Meerson, Phys. Rev. Lett. **107**, 180603 (2011).

[20] H. A. Kramers, Physica (Amsterdam) **7**, 284 (1940).

[21] P. Hänggi, P. Talkner, and M. Borkovec, Rev. Mod. Phys. **62**, 251 (1990).

[22] D. O. Harris, G. G. Engerholm, and W. D. Gwinn, J. Chem. Phys. **43**, 1515 (1965).

[23] R. P. Feynman and F. L. Vernon, Jr., Ann. Phys. (NY) **24**, 118 (1963).

[24] M. Thorwart, M. Grifoni, and P. Hänggi, Ann. Phys. (NY) **293**, 15 (2001).

[25] F. Chiarello, E. Paladino, M. G. Castellano, C. Cosmelli, A. D'Arrigo, G. Torrioli, and G. Falci, New J. Phys. **14**, 023031 (2012).

[26] L. F. Cugliandolo, C. R. Phys. **14**, 685 (2013).

[27] J. Eisert, M. Friesdorf, and C. Gogolin, Nat. Phys. **11**, 124 (2015).

[28] P. Facchi, S. Tasaki, S. Pascazio, H. Nakazato, A. Tokuse, and D. A. Lidar, Phys. Rev. A **71**, 022302 (2005); P. Caldara, A. La Cognata, D. Valenti, B. Spagnolo, M. Berritta, E. Paladino, and G. Falci, Int. J. Quantum Inf. **9**, 119 (2011).

[29] J. R. Friedman, M. P. Sarachik, J. Tejada, and R. Ziolo, Phys. Rev. Lett. **76**, 3830 (1996).

[30] P. T. Korda, M. B. Taylor, and D. G. Grier, Phys. Rev. Lett. **89**, 128301 (2002); K. C. Neuman and S. M. Block, Rev. Sci. Instrum. **75**, 2787 (2004).